

Random sequential adsorption of dimers on fractal structures

This article has been downloaded from IOPscience. Please scroll down to see the full text article.

1997 J. Phys. A: Math. Gen. 30 1925

(<http://iopscience.iop.org/0305-4470/30/6/018>)

View [the table of contents for this issue](#), or go to the [journal homepage](#) for more

Download details:

IP Address: 171.66.16.112

The article was downloaded on 02/06/2010 at 06:14

Please note that [terms and conditions apply](#).

Random sequential adsorption of dimers on fractal structures

M S Nazzarro, A J Ramirez Pastor, J L Riccardo and V Pereyra†

Department of Physics, Universidad Nacional d San Luis, Chacabuco y Pedernera, (5700) San Luis, Argentina

Received 29 October 1996

Abstract. We extend the study of diffusional relaxation on the random sequential adsorption of dimer introduced by Privman and Nielaba, to fractal media. The effect of added diffusional relaxation on the deposition of dimers in such disordered substrates makes full coverage in certain cases possible. We observe that in these cases, the limiting coverage is approached according to $t^{-d_s/2}$, where d_s is the spectral dimension of the substrate. The jamming coverage is analysed for different fractal substrates.

The deposition (or adsorption) of particles on solid surfaces is a subject of considerable practical importance. In many experiments on adhesion of colloidal particles and proteins on solids substrates the relaxation time scales are much longer than the times of the formation of the deposit.

A well known example of an irreversible monolayer deposition process is the random sequential adsorption (RSA). This process is well described in literature and has been investigated extensively in recent years [1–9]. The analysis of such phenomenon include theoretical studies, Monte Carlo simulations and experimental results, as, for example, the adhesion of latex spheres on a silica surface [10], which support the RSA model as possible theoretical tools to treat the irreversible adsorption. Exact solutions are possible, mainly for one-dimensional problems [1].

In a random sequential adsorption, objects of finite size are randomly deposited (adsorbed) on an initially empty d -dimensional substrate or lattice with the restriction that they must not overlap with previously added objects. The quantity of interest is the fraction of total area, $\theta(t)$, covered in time, t , by the depositing particles or objects. Due to the already randomly adsorbed particles blocking the area, the limiting or ‘jamming coverage’, θ_J , is less than that corresponding to the close packing ($\theta_J \equiv \theta(t = \infty) < 1$). The emergence of this jammed state is influenced by the infinite memory effects. Consequently, its formation cannot be described by the mean-field theory, except for very early times, when $\theta \propto t$.

The effect of diffusional relaxation on deposition have recently been [11, 12] analysed in random sequential adsorption of dimers in one-dimensional (1D) lattice. One of the main feature of added diffusional relaxation, in 1D, is to allow the full saturation coverage $\theta_J = 1$. Without diffusional relaxation the classical behaviour is recovered, where jamming

† To whom correspondence should be addressed.

coverage is given by $\theta_J = 1 - e^{-2} < 1$. The other important consequence of added diffusion to the dimer adsorption in 1D is that the final state is approached according to the $\propto t^{-1/2}$ power law preceded, for fast diffusion, by the mean-field crossover regime with intermediate $\propto t^{-1}$ behaviour, instead of the exponential approach for the pure adsorption case [1, 3].

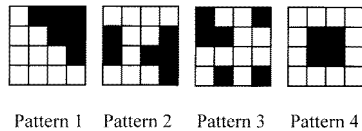
To explain such interesting behaviour, we can consider that the dominant effect of diffusion is to bring together single isolated vacancies in the late stages of the deposition. They can either be covered by an incoming dimer and disappear, or separated again due to diffusion. Thus, the process will reach its asymptotic long-time behaviour when most of the empty space is in single-site vacancies. The approach to the jamming coverage $\theta_J = 1$, for large times, will then be related to the diffusion-limited annihilation reaction $A + A \rightarrow \text{inert}$, with partial reaction probability upon each encounter of diffusing particles A , which represent the single-site vacancies. Such a reaction process is well described in literature and it turns out that the density of the surviving A -particles decreases as $\propto t^{-d_s/2}$ for large times, where d_s is the spectral dimension of the substrate [13]. It is also well known that a reduced reaction rate [14] allows the diffusion to mix the particles thus resulting in a mean-field behaviour for intermediate times, which in this case is $\propto t^{-1}$.

The analysis is also extended to the 1D k -mers deposition [15]. In this case the connection will be with the 1D diffusion-limited annihilation reaction $kA \rightarrow \text{inert}$. By using scaling arguments it is possible to conclude that the density will follow the mean-field law $\propto t^{-1/(k-1)}$ for large times and $k > 3$, with possible logarithmic corrections for $k = 3$.

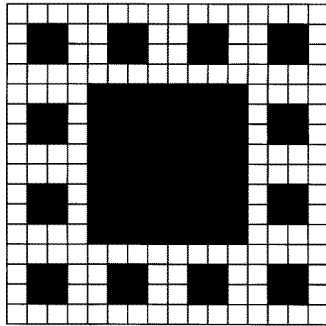
Despite the connection between the diffusion-limited annihilation reaction and the effect of diffusion in 1D k -mers deposition, the argument cannot be generalized to higher euclidean dimensions. In fact, in the case of RSA of lattice hard squares in two dimensions with diffusional relaxation the approach to the full coverage $\theta_J = 1$ is given by the power law $\propto t^{-1/2}$. The same behaviour is observed in the deposition of 2×2 square objects on a two-dimensional (2D) square lattice where the full coverage is reached [16]. No studies have been carried out along these lines for deposition on fractals. It is then interesting to determine whether the argument which connects the diffusion-limited annihilation reaction with the diffusional relaxation on the dimer deposition is valid on fractal substrates embedded in 2D. In order to elucidate the problem we generalize the study of added diffusional relaxation to the dimer deposition on different fractal substrate with fractal dimension between $1 < d_f < 2$.

The fractals we have studied in this work are two well differentiated structures, the first one is the well known probabilistic diffusion-limited aggregation (DLA) clusters [17], with $d_f = 1.72$, $d_w = 2.86$ and $d_s = 1.20$; the others belong to the 2D Sierpinski carpet family [18]. The advantage with the latter group, is that they can be easily generated on the computer and d_f , d_w and d_s can be suitably varied. The generation of the patterns is shown in [19]; here we describe briefly the method. A square is divided into m equal units each corresponding to a site on a square lattice. A certain number, say l of these are blocked, leaving $k = m - l$ accessible sites. The connectivity with all the sides of the square must be guaranteed. This is the basic unit which is repeated self-similarly in subsequent stages. The Hausdorff dimension of these patterns is $d_f = \ln(k)/\ln(s)$, where s is the scaling factor. Since d_f is given basically by the number of accessible sites and the scaling factor, a number of different patterns can be easily generated by this method. Figure 1 shows the basic units of the patterns that we have used in our study. The others quantities which characterize the fractal structures, d_w and d_s are obtained as the exponent of the mean square displacement covered by a random walker and the number of the distinct sites visited as a function of time, respectively.

After the generation of the substrate we proceed to simulate the RSA process with



(a)



(b)

Figure 1. (a) Basic units of Sierpinski carpets. The scaling factor is 4. (b) The second stage of the generation of the carpet, here the unit pattern is 4. Open squares represent allowed sites.

diffusional relaxation. At each Monte Carlo step a pair of neighbouring sites are chosen at random, then a decision is made about what type of process will take place: (i) deposition with probability p ; (ii) diffusion with probability $1 - p$, where $0 < p \leq 1$. Note that, the case $p = 1$ is the pure RSA process.

If the deposition attempt is chosen, then the sites are occupied provided that both of them are empty, otherwise the attempt is rejected.

If the diffusion attempt is selected, we test whether both sites are occupied for the same dimer. The diffusion step proceeds as follows (see figure 2): The number, ' n ', of the nearest-neighbour sites of both component of the dimer which belong to the fractal structure is determined. This number can be $n = 1, \dots, 6$. Then the movement is selected as follows. One of the ' n ' possibilities is chosen at random. If the selected site is covered by a particle the attempt is rejected. Otherwise it turns out that one of the component of the dimer's heads is moved over the empty site by conserving the dimer bond length. Actually, this can be accomplished by rotating the dimer around an axis normal to the lattice passing through the dimer's fixed head. Thus, this relaxation mechanism enables the dimer to change its direction during diffusion on the surface. It should be noticed that alternative diffusion mechanisms, such as translation along the dimer's axis are naturally embodied. The proposed diffusion method was recently introduced by Wang and Fichthorn [21] to analyse the movement of homonuclear dimers adsorbed on sc(100) and fcc(100) surfaces.

As in [11], the dimensionless Monte Carlo time variable, t , may therefore be defined by having one attempt per lattice site in the unit time step $\Delta t = 1$. Thus, for the N -site lattice, the time step $\Delta t = 1$ corresponds to N deposition/diffusion attempts Monte Carlo steps described earlier. Another convenient definition is the time variable $\tau = pt$ which corresponds to the fixed deposition attempt rate [11]. Under this definition the diffusion attempt is proportional to $(1 - p)/p$.

In order to analyse the effect of the diffusional relaxation on the deposition process,

Diffusional Relaxation Mechanism

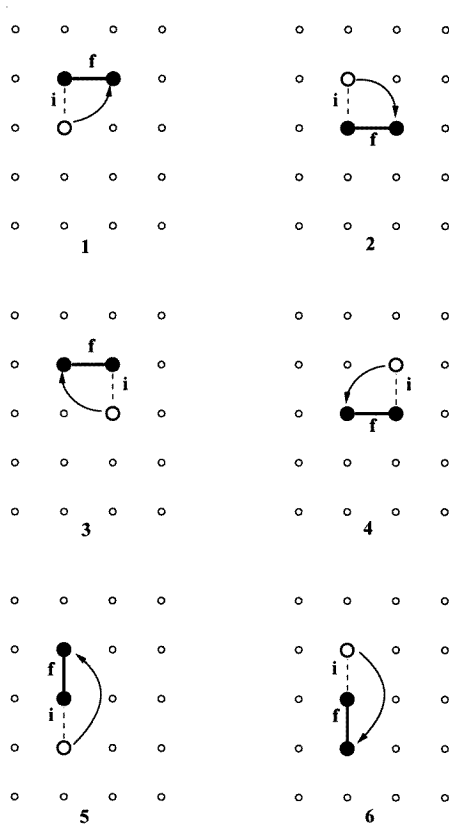


Figure 2. Diffusion mechanism used in the relaxation. All possible transitions on a square lattice are shown; 'i' and 'f' denote the initial and final state respectively.

Monte Carlo simulations were performed for different values of the parameter p . The number of sites for the fractal structures analysed here were typically of 10^5 sites (typically this corresponds to five generations for the Sierpinski structures P1, P2, P3 and P4 with $s = 4$). Each data set was averaged over 500 runs. All the numerical calculations were carried out at a PARIX parallel computer system with eight nodes.

The first structure that we have considered in our analysis is the DLA clusters. In figure 3, we observe the numerical results of the coverage $\theta(t)$ plotted as a function of $\ln(pt)$, for different values of the probability p . The pure RSA process onto the DLA structure, $p = 1$, gives a jamming coverage $\theta_J = 0.8245$. The approach to this final state (asymptotic regime) obeys a clear exponential law, as in the 1D case. The addition of diffusion to the adsorption process gives as a result a jamming state with jamming coverages $\theta_J = 0.9303$.

Since relaxation to jamming state may be driven by slowly decaying fluctuations, (see figure 3) the jamming coverage was obtained by extrapolating the dependence of $\theta(t)$ versus $1/\ln(pt)$ for $t \rightarrow \infty$.

Since for any configuration of dimers on the DLA the diffusion mechanism allows for

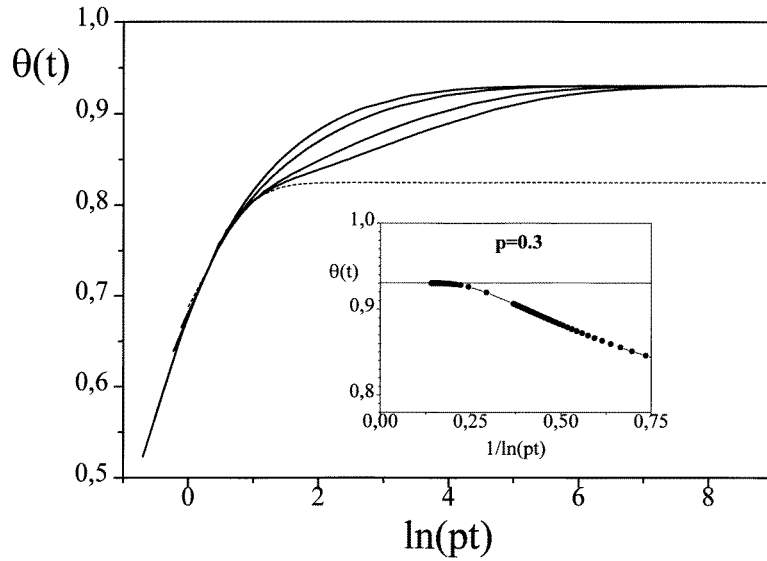


Figure 3. Numerical results of coverage $\theta(t)$ versus $\ln(pt)$ for a DLA. The full curve represents diffusion relaxation and various values of p ($p = 0.1, 0.3, 0.8, 0.9$) (it curves from top to bottom corresponding to increasing values of p); the dotted curve represents pure adsorption. The inset shows $\theta(t)$ versus $1/\ln(pt)$ used to calculate θ_J by extrapolation.

all possible transformations between the filled-sites and the empty-sites sets this asymptotic coverage corresponds to the maximum coverage attainable on the given fractal structure.

In figure 3, it can be seen that the full coverage, $\theta_J = 1$ is never reached on the DLA cluster, even by allowing diffusional relaxation.

In figure 4, the asymptotic regime, for the DLA cluster is shown for various values

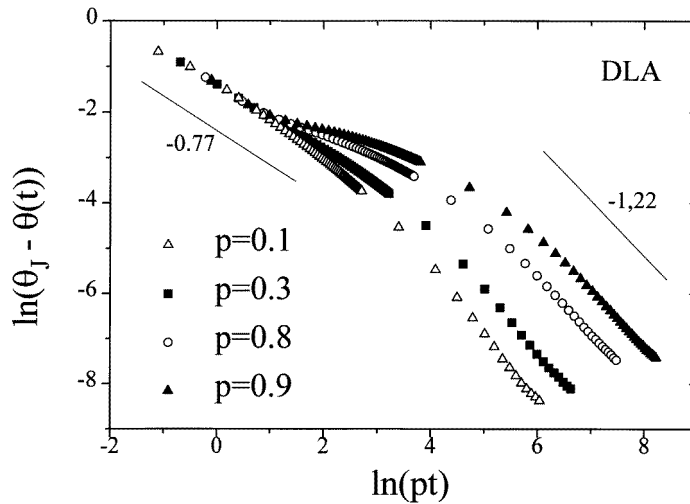


Figure 4. Idem figure 3 for long times, plotted as $\ln[\theta_J - \theta(t)]$ versus $\ln(pt)$, for different values of p .

of p . As we observe, the limiting coverage is approached according to the power law $[\theta_J - \theta(t)] \propto t^{-\alpha}$ with $\alpha = 1.22 \pm 0.03$ which comes close to the spectral dimension of the cluster $d_s = 1.20$. We can also observe that the asymptotic regime is preceded by an intermediate time behaviour which is also a power law, $\propto t^{-0.77}$ different from the 1D mean-field intermediate decay $\propto t^{-1}$ behaviour. This is merely a consequence of local inhomogeneities in the connectivity of the DLA sites which hinders a continuous filling of the structure with dimers.

The asymptotic time behaviour of the RSA of dimers with diffusional relaxation on DLA cluster is one of the most interesting features of the process. The power-law exponent is two times the value of the exponent of density decay in the diffusion-limited annihilation reaction $A + A \rightarrow \text{inert}$ on this structure. Also the intermediate time regime does not follow a mean-field behaviour. Certainly, the mechanism of the diffusional relaxation is probably modified by the presence of a considerable number of inaccessible sites which exist in the dangling ends and backbends of the structure. We can conclude that the connection between RSA with diffusional relaxation and the diffusion-limited annihilation reaction, which is completely valid in 1D, is not valid on the DLA clusters.

Deterministic fractals, as we described above, belong to the Sierpinski carpet family. Different patterns (see figure 1) have been used to analyse the RSA process of dimers. The effect of diffusion relaxation on the RSA process, is also analysed for these structures. Free boundary conditions have been imposed in the DLA structure as well as in all Sierpinski fractals used in the simulation. Since the number of generations of the deterministic fractals used in simulations was very large, no finite size effect is observed in the jamming coverage and kinetics.

In tables 1–3 we have shown different parameters, which characterize fractal structures, such as the average number of nearest neighbours per site, η , Hausdorff dimension, d_f , spectral dimension, d_s , and jamming coverage, θ_J , obtained for $p = 1$ (without relaxation). As we can observe in table 1, there is not a clear dependence of θ_J on the other parameters.

Table 1. Different characteristic parameters for DLA and Sierpinski structures ($s = 4$).

Substrate	θ_J	η	$d_s/2$	d_f
DLA	0.8245	2.22	0.60	1.72
P1	0.7896	2.64	0.55	1.66
P2	0.7711	2.36	0.60	1.66
P3	0.7832	2.22	0.61	1.66
P4	0.8952	2.96	0.72	1.79

Table 2. Different characteristic parameters for the fractal generated by pattern 4, upon changing the relationship between k and s .

P4	θ_J	η	$d_s/2$	d_f
3×3	0.8885	3.18	0.77	1.89
4×4	0.8952	2.96	0.72	1.79
5×5	0.8938	2.88	0.71	1.72
6×6	0.8936	2.78	0.68	1.67
7×7	0.8933	2.75	0.68	1.63
8×8	0.8939	2.73	0.67	1.60
9×9	0.8947	2.72	0.60	1.58

Table 3. Idem table 2, by using pattern 1.

P1	θ_J	η	$d_s/2$	d_f
2×2	0.6501	2.00	0.44	1.58
3×3	0.8109	2.40	0.62	1.63
4×4	0.7896	2.67	0.57	1.66
5×5	0.8279	2.86	0.63	1.68
6×6	0.8325	3.00	0.63	1.70
7×7	0.8444	3.11	0.64	1.71
8×8	0.8511	3.20	0.58	1.72

In table 2, we have calculated the characteristic parameters using the same pattern (P4) and changing the relation between k and s to generate the fractal structures, in this way, fractal dimension, d_f , spectral dimension, d_s and the parameter η decrease as the size of the basic unit increases, however, the jamming coverage, θ_J , is almost constant. It is interesting to note that the value of $\theta_J \approx 0.895$ for this fractal structure (P4) is close to the value of the square cactus $\theta_J = 0.8946$ [20].

In table 3, we have shown the same study for the fractal generated by using pattern 1, as we observe, θ_J increases with the fractal dimension. In all the cases, we observe that there is not a clear relationship between the jamming coverage and the different characteristics of the substrate.

Actually, the maximum coverage allowed for structures generated from patterns 1, 2 and 3, upon an ordered way of filling sites with dimers, is found to be $\theta_J = 0.8$ by simple inspection. However, structure generated from pattern 4 can be completely covered, say $\theta_J = 1.0$.

The analysis of the large-time behaviour for the patterns 1, 2 and 3 gives a power-law exponent α , which is far from $d_s/2$. As an example, in figure 5 we have shown the asymptotic regime for the structure P2, for different values of the probability p , the best fitting parameter obtained is $\alpha = -1.52$ (here $d_s/2 = 0.6$).

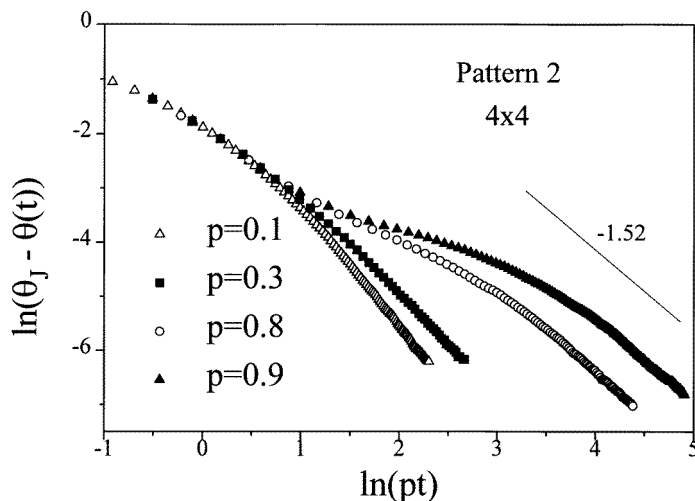


Figure 5. Idem figure 4 for pattern 2 (P2); $\theta_J = 0.8$ for this case.

Provided that full coverage is reached in the structure generated by using pattern 4, we considered the case P4 in detail. In figure 6, we can observe the numerical results for the coverage for large times, plotted as $\ln[\theta_J - \theta(t)]$ versus $\ln(pt)$, for $p = 0.1, 0.3, 0.8, 0.9$. The size of the unit cell used was 4×4 . From the slope of the curve we can obtain the exponent of the power law which approached $\alpha = 0.72$ in agreement with the value $d_s/2$. This result is in accordance with the argument of Privman and Nielaba [11] which states that the density of the surviving particles (empty sites) ρ , on fractal substrate decreases as $\rho \propto t^{-d_s/2}$. In order to confirm this speculation we varied slightly the spectral dimension of the fractal structure by changing the scaling factor from $s = 4$ to $s = 3$, in this way d_s changes from $d_s/2 = 0.72$ to $d_s/2 = 0.77$, respectively. It should be noticed that this small change varies the slope of the long-time regime (see figure 7), so that the agreement

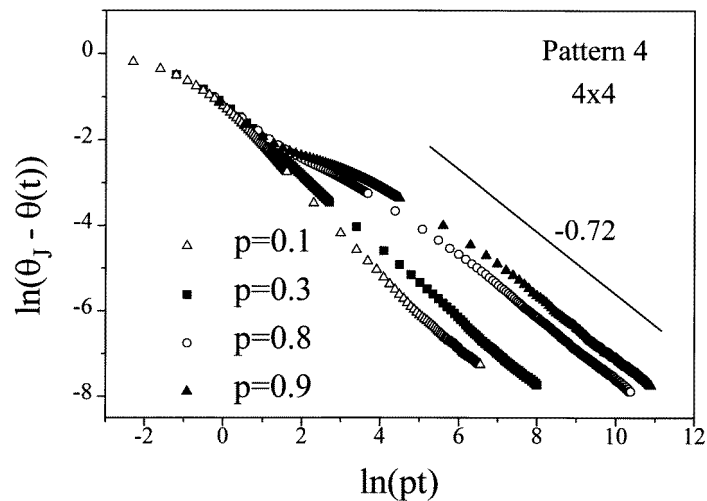


Figure 6. Idem figure 5 for pattern 4 (P4) ($s = 4$). Particularly, $\theta_J = 1.0$ for this case.

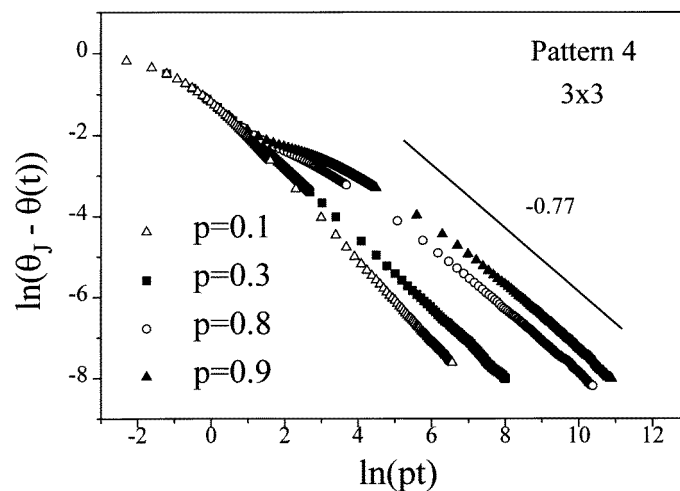


Figure 7. Idem figure 6 for $s = 3$.

$\alpha = d_s/2 = 0.77$ is recovered again. This result reinforces that the argument $\rho \propto t^{-d_s/2}$ is valid for fractal structure which can be fully covered by the deposition-diffusion mechanism. It is important to emphasize that exponent α describes the kinetics at short and long times. At intermediate times a well determined crossover region appears as p increases.

As a conclusion, in this work we have studied the random sequential adsorption of dimers on different fractal structures embedded in 2D. We observe that there is not a relationship between the jamming coverage and the different characteristic parameters of the substrate. The effect of added diffusional relaxation to the deposition process, allows full coverage in certain structures, only in these cases is it possible to confirm the argument of [11], that is, the empty sites fraction decay as $[\theta_J - \theta(t)] \propto t^{d_s/2}$. However, this rule does not hold for structures where full coverage cannot be reached, as for instance the DLA, P1 P2 and P3, structures for which the exponent of the power law differ significantly from the value of $d_s/2$. Particularly, for DLA $[\theta_J - \theta(t)] \propto t^{-\alpha}$ with $\alpha \approx d_s$. It appears that the set of inaccessible sites in a given structure promotes local density inhomogeneities (fluctuations) that are slowly smeared out, hence slowing down the time relaxation to maximum coverage. It is known from the $A + A \rightarrow$ inert reaction kinetics that the long-time decay is mainly dependent on the local density inhomogeneities. Accordingly, geometrical constraints of the structure leading to local density fluctuations are expected to have a predominant influence on the long-time kinetics of dimers onto it.

Acknowledgments

This work was partially supported by the Consejo Nacional de Investigaciones Científicas y Técnicas and Fundacion Antorchas (Argentina). The European Economic Community, Project ITDC-240, is greatly acknowledged for the provision of valuable equipment.

References

- [1] Evans J W 1993 *Rev. Mod. Phys.* **65** 1281
- [2] Bartelt M C and Privman V 1991 *Int. Mod. Phys. B* **5** 2883
- [3] Gonzalez J J, Hemmer P C and Hoye J S 1974 *Chem. Phys.* **3** 228
- [4] Privman V, Wang J-S and Nielaba P 1991 *Phys. Rev. B* **43** 3366
- [5] Evans J W and Nord R S 1985 *J. Stat. Phys.* **38** 681
- [6] Talbot J, Tarjus G and Schaaf P 1989 *Phys. Rev. A* **40** 4808
- [7] Schaaf P and Talbot J 1989 *Phys. Rev. Lett.* **62** 175
- [8] Viot P, Tarjus G and Talbot J 1993 *Phys. Rev. E* **48** 480
- [9] Renyi A 1963 *Sel. Trans. Math. Stat. Prob.* **4** 205
- [10] Onoda G Y and Linigier E G 1986 *Phys. Rev. A* **33** 715
- [11] Privman V and Nielaba P 1992 *Europhys. Lett.* **18** 673
- [12] Bonnier B and McCabe J 1994 *Europhys. Lett.* **25** 399
- [13] Ben-Avraham D, Burschka M A and Doering C R 1990 *J. Stat. Phys.* **60** 695
Ben-Avraham D and Doering C R 1988 *Phys. Rev. A* **37** 5007
- [14] Braunstein L, Martin H O, Grynberg M and Roman H E 1992 *J. Phys. A: Math. Gen.* **25** L255
- [15] Nielaba P, Privman V and Wang J-S 1991 *J. Phys. A: Math. Gen.* **23** L1187
Nielaba P and Privman V 1992 *Mod. Phys. Lett. B* **6** 533
- [16] Nielaba P, Privman V and Wang J-S 1994 *Ber. Bunsenges. Phys. Chem.* **98** 451
- [17] Witten T A and Sander L M 1981 *Phys. Rev. Lett.* **47** 1400
- [18] Mandelbrot B B 1977 *Fractals, Form, Chance and Dimension* (San Francisco, CA: Freeman)
- [19] Dasgupta R, Ballabh T K and Tarafdar S 1994 *Phys. Lett. A* **187** 71
- [20] Evans J W and Nord R S 1985 *Phys. Rev. B* **31** 1759
- [21] Wang J C and Fichtorn K 1996 *Langmuir* **12** 139